International Journal of
Plasma Environmental Science and Technology

Regular Paper DOI: 10.34343/ijpest.2024.18.e01001

Ammonia decomposition over Ce and La-based materials in an electric field

Valeriia Maslova[1], Elodie Fourré[1], André Grishin[2], Gleb Veryasov[2], Catherine Batiot-Dupeyrat[1,*]

[1] IC2MP, ENSIP, Université de Poitiers - UMR CNRS 7285, 1 rue Marcel Doré, TSA 41105, 86073 Poitiers cedex 9, France
[2] TotalEnergies One Tech Belgium Zone Industrielle C7181-Feluy, Belgium

* Corresponding author: catherine.batiot.dupeyrat@univ-poitiers.fr

Received: 25 November 2023
Revised: 19 December 2023
Accepted: 25 December 2023
Published online: 5 January 2024

Abstract

Ammonia decomposition into hydrogen and nitrogen was performed under electric-field in a point to plane reactor at ambient temperature and pressure. A set of four catalysts presenting various structures, namely cerium dioxide (CeO_2) and lanthanum oxide (La_2O_3), along with cerium phosphate ($CePO_4$) and cerium zirconate ($CeZrO_4$), were assessed for their efficiency in the reaction. The best results in terms of activity, expressed as the number of mole of ammonia decomposed per weight of catalyst, were obtained with $CePO_4$, followed by $CeZrO_4$, CeO_2 and La_2O_3. It corresponds to the material possessing the highest pore volume and the lowest permittivity.

Keywords: Ammonia, electric field, catalyst.

1. Introduction

Hydrogen is considered as an excellent energy carrier due to its carbon-free and environmentally friendly features [1, 2]. It plays a crucial role in the current energy transition. However, traditional methods of hydrogen production, such as steam methane reforming, are energy-intensive and emit greenhouse gases. Ammonia decomposition has emerged as a promising alternative, since no carbon dioxide is emitted and ammonia is easier to liquify and store than hydrogen [3, 4]. In fact, an alternative to the conventional storage of hydrogen as a compressed gas is chemical storage. In this approach, hydrogen is produced on-site through a chemical reaction involving a hydrogen-containing compound. Within the range of available hydrogen carrier molecules (such as liquid organics or methanol), ammonia decomposition surpasses other systems due to its high hydrogen capacity (17.7 wt%). The decomposition of ammonia emerges as one of the most promising method to produce “clean” hydrogen. It is an endothermic reaction:

$$2NH_3 \rightarrow 3H_2 + N_2 \qquad (\Delta_r H° = 91.2 \text{ kJ mol}^{-1}) \qquad \text{(R1)}$$

Industrially, the conditions to crack ammonia are about 850−950 °C with nickel supported on alumina catalyst, which is mechanically strong and heat resistant [5]. Silva *et al*. [6] achieved NH_3 conversion > 99% with a Fe-Ni/Al_2O_3 catalyst at a temperature of 650 °C. Ruthenium supported on MgO is also proposed as efficient catalyst (> 98 %) at a more moderate temperature (425 °C) [7]. However, Ru high cost hinders its commercial development.

In the pursuit of finding alternative activation methods at low temperature, non-thermal plasma coupled to catalysis appears as an ideal solution for both ammonia synthesis and decomposition [8]. Recently, a system was proposed using a packed-bed dielectric barrier discharge reactor at room temperature [9] and a NH_3 conversion of 15% was achieved with $MgAl_2O_4$ for a deposited power of 21 W. Besides plasma, the use of a DC electric field (EF) over a catalyst bed (without dielectric barrier) appears as an interesting process to

perform several reactions such as ammonia synthesis. Sekine's group [10] attributed the enhancement of products yield to surface protonic conductivity. The advantage is that EF requires lower deposited power than classical DBD plasma reactor. However, it has been shown that the electrical conductivities of catalysts impact the reaction field type. For example, a plasma reaction occurs in presence of lanthanum oxide. In contrast, catalysts with electrical conductivities, such as Sr-doped La_2O_3 or CeO_2, do not generate plasma, but maintain a catalytic reaction through an electric field [11].

Recently, we demonstrated that Fe and Ru deposited on CeO_2 catalysts present activity in the decomposition of NH_3 in an electric field [12]. In this study ammonia decomposition was investigated under EF for a series of Ce-based materials and compared with La_2O_3.

2. Experimental

2.1 Reactor configuration

The ammonia decomposition reaction in electric field was carried out in a reactor with a point-to-plane configuration (Fig. 1). A sharp tungsten electrode of 0.5 µm-diameter point was set as the high voltage electrode. The distance between the tip of the tungsten electrode and metallic fritted one was fixed at 2 mm distance inside a Teflon connector (i.d. 4 mm). The catalyst grains, sieved in the 355/630 µm range, filled the volume of 2 mm height between the electrodes. A DC high-voltage power supply (SPELMAN, SL300) was used.

The reaction was conducted at ambient temperature and pressure at a fixed current value (4, 6 and 8 mA) while the voltage required to maintain the current varied. The weight of catalyst was between 30 and 80 mg in order to fill the space between the two electrodes.

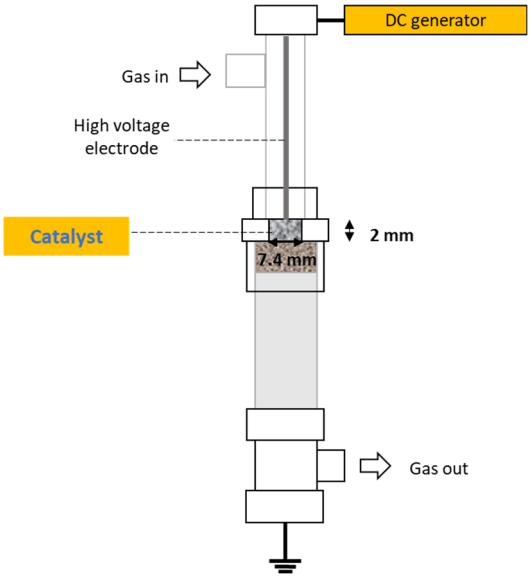

Fig. 1. Schematic representation of the reactor.

2.2 Experimental setup overview

The reaction was performed using a mixture of ammonia diluted in helium (5 vol% of NH_3). The gaseous product of reaction (essentially N_2, H_2) and unconverted ammonia was analyzed in situ by a micro GC Varian gas chromatograph equipped with a CP-Volamine column (Agilent) using He as carrier gas.

CeO_2 and La_2O_3 were commercial powders while other catalysts were synthesized in the laboratory. The preparation of $CePO_4$ was based on hydrothermal method reported elsewhere [13]. Ceria-zirconia mixed oxides were prepared by classical sol-gel method using nitrate as precursor salt [14].

Efficiency of the process was calculated as follows (Eq. 1):

$$\text{Efficiency}\left(\frac{\text{mmol}}{\text{kJ}}\right) = \frac{[Q_i\left(\frac{\text{mol}}{\text{min}}\right) - Q_f\left(\frac{\text{mol}}{\text{min}}\right)] \times 10^6}{60 \times \text{Power (W)}} = \frac{1}{\text{SER}} \quad (1)$$

Where Power (W or J s^{-1}) is the product of deposited voltage (kV) by current (mA), and Q_i and Q_f are the initial and final molar fluxes of ammonia in feed.
SER: Specific Energy Required

The catalyst activity was normalized per mass of catalyst according to Eq.2. It corresponds to the space time yield (STY) as proposed by Kim *et al*. [15].

$$\text{STY}\left(\frac{\text{mol}}{\text{h} \times \text{g}_{\text{cat}}}\right) = 1000 \times \frac{\text{Converted NH}_3(\frac{\text{mol}}{\text{h}})}{\text{mass of catalyst (g)}} \quad (2)$$

Permittivity was determined using Impedance Spectroscopy Measurements with a Modulab Solartron Analytical potentiostat in a 1−10 MHz frequency range. A 1 V amplitude alternating signal was applied, with respect to the system linear behaviour. A two electrode configuration at room temperature in ambient air was used. The sample was introduced as pellet of 3 cm of diameter and 0.558–1.335 mm of thickness, pressed by applying 5 tons of force, and dried at 40 °C in the oven during 48 hours. The pellet was placed between two flat copper current collectors playing the role of electrodes, one of which is a guard electrode of 2 cm (3.1415 cm^2). The thickness of each sample was measured systematically by the instrumentation installed into sample holder (Solartron) and automatically normalised so that to minimize the geometrical factor.
The permittivity was found by extrapolating at 10 MHz frequency relying on a simple capacitor model (Eq.3)

$$\varepsilon = \frac{\text{C} \times \text{L}}{\varepsilon 0 \times \text{A}} \quad (3)$$

where C is a capacitance automatically calculated with respect to sample thickness (L), and the surface of guard electrode A.

XRD analyses of the samples were carried out on diffractometer Malvern Panalytical®, Empyrean model. The source is a copper tube working with a voltage of 45 kV and a current of 40 mA. Diffractograms were recorded in the range of 10–100° (2θ) with a step of 0.01°. Particle size determination was done by Scherrer equation over the 100% peak. The specific surface area and pore volume of materials were measured by N_2 physisorption technique at 77 K using TriStart 3000 Micromeritics instrument, applying single point BET analysis (Brunauer–Emmett–Teller). The morphology at a microscopic scale of $CePO_4$ and $CeZrO_4$ samples was examined using Scanning Electron Microscopy instrument SEM FEG JSM-7900F Jeol (5 kV, SEI detector and 6 mm working distance).

3. Results

The catalysts were characterized using conventional techniques such as X-Ray Diffraction (XRD), N_2 physisorption, and Scanning Electron Microscopy (SEM). The results reported in Table 1 show that both CeO_2 and La_2O_3 have low surface area while $CePO_4$ and $CeZrO_4$ exhibit a surface area of 37 and 34 $cm^3\ g^{-1}$, respectively.

The materials differ significantly in terms of pore sizes. The commercial CeO_2 is a non- porous solid. The porosities of $CePO_4$ and La_2O_3 are similar with values of 0.10 and 0.09 $cm^3\ g^{-1}$, respectively. SEM analysis of $CePO_4$ (Fig. 2) and $CeZrO_4$ (Fig. 3) reveal different morphologies. The presence of nanorods is clearly visible for $CePO_4$ similar to what was reported by Sato *et al*. [16].

Decomposition of ammonia was investigated over CeO_2 at different fixed current values: 4, 6 and 8 mA. Fig. 4 shows the evolution of conversion in time at different applied currents.

Table 1. Characterization of the material by N_2 physisorption.

Catalyst	d_{crys} (nm)	S_{BET} (m^2 g^{-1})	V_{pore} (cm^3 g^{-1})
CeO_2	77	2	–
$CePO_4$	18	37	0.10
$CeZrO_4$	6	34	0.06
La_2O_3	70	3	0.09

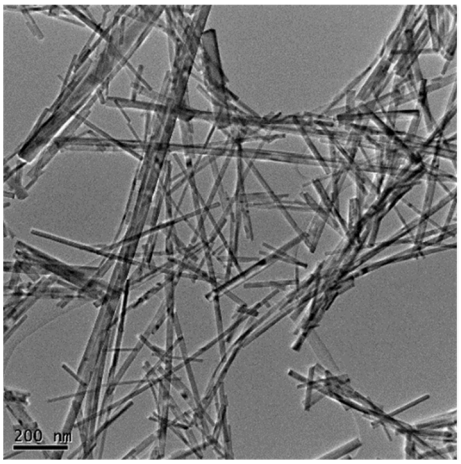

Fig. 2. SEM image of the monoclinic $CePO_4$.

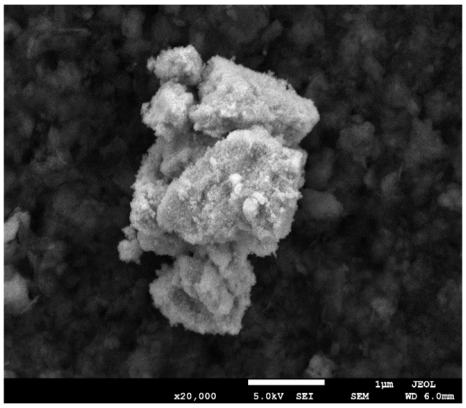

Fig. 3. SEM image of $CeZrO_4$.

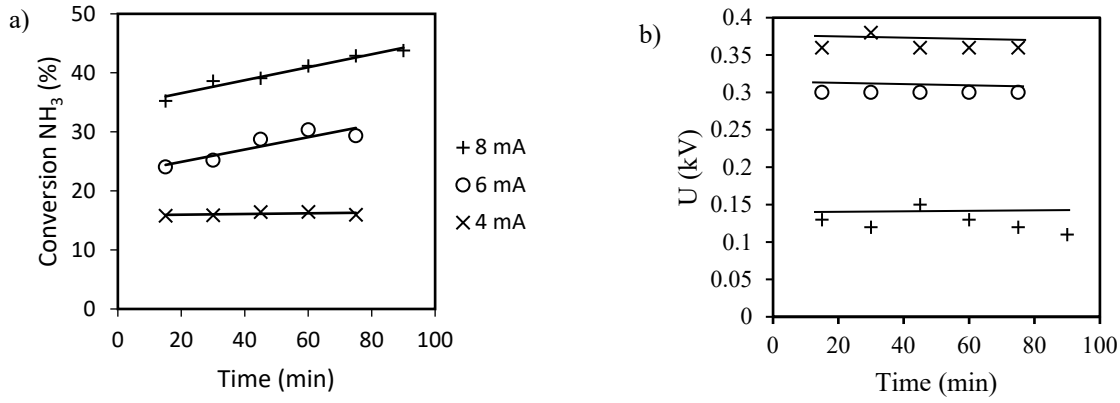

Fig. 4. Ammonia decomposition over CeO_2 catalyst, 5% NH_3/He, 30 mL min^{-1} total flow, ambient conditions a) NH_3 conversion versus time for i = 4, 6 and 8 mA, b) imposed voltage for input current i = 4, 6, 8 mA.

The NH_3 conversion is stable in time at 4 mA, while an increasing tendency is observed, with an improvement in efficiency at 6 and 8 mA. The results in Fig. 4 (b) show that with the increase of the input current, the imposed voltage decreased, suggesting the creation of a greater amount of active species in gas phase or on the surface of CeO_2 which could sustain the electric field. Moreover, it was shown that ammonia was converted only into nitrogen and hydrogen, and no other by-products were produced such as hydrazine, as obtained in other published paper [17].

La_2O_3 and CeO_2 activities were compared as they possess similar specific surface areas (Fig. 5). One can see that there is no substantial difference in conversion of ammonia between the two catalysts, and a small decrease in efficiency could be observed.

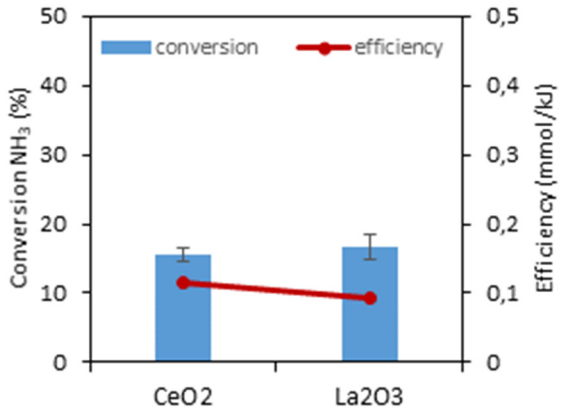

Fig. 5. Ammonia decomposition over La_2O_3 and CeO_2 catalyst. 5%NH_3/He, 30 mL min^{-1} total flow, ambient conditions; 4 mA.

Comparison of voltage data for both catalysts, shown on Fig. 6, reveal a greater voltage for La_2O_3. This can be explained by the fact that La_2O_3 is generally characterized by a lower conductivity compared to CeO_2 [18, 19].

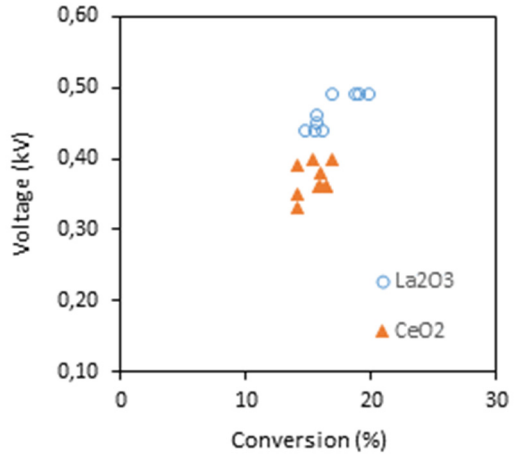

Fig. 6. Dependency of voltage vs. conversion for La_2O_3 and CeO_2 catalyst. Conditions: 5%NH_3/He, 30 mL min^{-1} total flow, ambient conditions; 4 mA.

The Ce-based catalysts are compared in Fig. 7 at a fixed current of 8mA. The results show that CeO_2 is the most active catalyst within the Ce-based materials tested. The operating voltage to maintain the current at 8mA differ slightly for the three materials, it is comprised between 0.36 and 0.46 kV (Table 2). The lowest value is obtained for the semiconductor CeO_2. No direct correlation is visible between permittivity and operating voltage but the three materials are characterized by low dielectric constant.

Another important point to note is that the amount of catalyst used to completely fill the zone between the two electrodes differ strongly from one material to another.

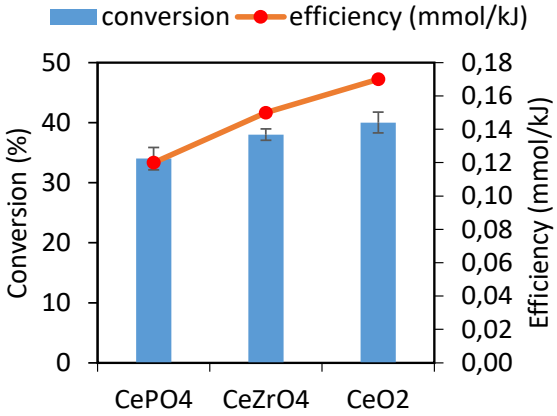

Fig. 7. Ammonia decomposition over Ce-based catalyst. 5%NH_3/He, 30 mL min^{-1} total flow, ambient conditions; 8 mA.

The activity of catalysts was then normalized per mass of catalyst (Eq. 2). The results, gathered in Table 2, show that $CePO_4$ is the best catalyst in terms of mol of ammonia decomposed per gram of catalyst and per hour (space time yield). The low amount of catalyst used to fill up the catalytic zone is due to the low bulk density of $CePO_4$ compared to $CeZrO_4$ and CeO_2. The highest activity is reached with the catalyst possessing the lowest permittivity. It corresponds also to the material with the highest porosity.

Table 2. Weight of catalyst and space time yield (STY) of catalyst over Ce-based catalyst. 5%NH_3/He, 30 mL min^{-1} total flow, ambient conditions; 8 mA.

Catalyst	Permittivity	U (kV)	Weight (mg)	STY (mol $h^{-1}g^{-1}$)
CeO_2	6.5	0.36	80	16.8
$CeZrO_4$	6.5	0.46	65	21.6
$CePO_4$	4.2	0.42	31	34.2

4 Discussion

Cerium oxide and lanthanum oxide are two commonly used rare earth metal oxides that serve as supports for metals in traditional thermal catalysis for ammonia decomposition [20]. We show here that these two oxides are active in ammonia decomposition at room temperature under electric field without the need of metal species supported at the oxide surface. Over CeO_2, NH_3 conversion increases with time for 6 and 8 mA which is not the case for 4mA. Moreover, it is shown that the voltage is not increased, it proves that a modification of the electric field is not responsible for the conversion increase. It could be due to an increase in crystal size or the formation of defects in the structure of CeO_2 when a higher current is applied. Indeed, cerium oxide is known to possess oxygen vacancies that could be modified with time at higher applied current [21].

Both CeO_2 and La_2O_3 exhibit similar ammonia conversion rates at a fixed current of 4 mA, despite their very low surface areas. However, the energy efficiency, expressed in mmol of NH_3 decomposed per kJ, although low for the two materials, is higher for CeO_2 due to its lower operating voltage at 4 mA. This lower voltage is attributed to the higher conductivity of CeO_2 compared to La_2O_3. Indeed, it is believed that the low conductivity of La_2O_3, characteristic of a dielectric material, leads to the formation of a spark discharge. Conversely, CeO_2, being a semi-conductor type material, does not favour plasma formation [11].

As suggested by Sekine's group [22], the reaction mechanisms under electric field is significantly different from the conventional thermo catalytic reactions. Adsorbed species play a key role for proton hopping on the catalyst surface, with or without metal species deposited at the surface of the catalyst. An associated reaction mechanism is proposed under electric field in which N_2 dissociate via the formation of N_2H^+ as intermediate promoted by proton hopping.

Despite their markedly different morphologies revealed by SEM analysis, $CePO_4$ and $CeZrO_4$ exhibit comparable NH_3 conversion, suggesting that these properties do not directly influence the catalytic activity. However, the three Ce-based materials show distinct redox properties. In classical catalysis the defects in CeO_2 associated with the Ce^{3+}/Ce^{4+} couple contribute to its superior catalytic performance. $CeZrO_4$ possesses also oxygen vacancies, while Ce maintains a stable oxidation state as Ce^{3+} in $CePO_4$ [23]. In contrast to pure thermo catalytic process, it is evident that the presence of defects in the solid structure does not significantly impact ammonia decomposition.

Under electric field, the imposed voltage does not follow the Ohm's low (U = R I) as shown in Figure 4b). Over CeO_2 an increase of the applied current leads to a significant decrease of the imposed voltage as shown also by Oshima *et al*. [24]. Comparing $CePO_4$, $CeZrO_4$ and CeO_2, the lowest value of imposed voltage was reached for CeO_2, which exhibits also the higher activity. It is believed that the imposed voltage is dictated by the gas atmosphere and the electrical conductivity of the catalyst. Consequently, it appears that the conversion of ammonia depends on the nature of the catalyst stronger than on the effect of the electric field.

The catalytic activity normalized per mass of catalyst is the highest with $CePO_4$, which is associated to its larger pore volume (0.10 $cm^3\ g^{-1}$) as shown in table 1. However, it is challenging to definitively attribute the enhanced performances only to this parameter. Permittivity, a physical parameter that reflects the polarizability of the catalyst and the interfacial space charge, should also be considered. Based on calculations, it was reported that the propagation of discharge inside pores is defined by the permittivity of materials [25]. Moreover, it has been observed that solids with low permittivity exhibit higher activity in plasma-catalysis process compared to those with higher permittivity values.

The experimental results obtained in this study match with the proposed explanations. Nevertheless, the catalyst with the highest pore volume and lowest permittivity consistently demonstrates superior performance, making it difficult to identify the exact role of each parameter. Further studies are required to gain a more comprehensive understanding of the parameter that plays the most significant influence on the activity.

5. Conclusion

This study demonstrates the feasibility and the energy efficiency of ammonia decomposition using the electric field process at ambient temperature and pressure and over Ce- and La-based catalysts. As expected, increasing the applied current with CeO_2 catalyst leads to a higher NH_3 conversion. At a fixed current of 4mA, CeO_2 shows the highest NH_3 conversion among the tested catalysts, while $CePO_4$ demonstrates the highest activity, normalized per mass of catalyst.

Further investigations are necessary to gain a deeper understanding and improve the reaction of ammonia decomposition under electric field.

Acknowledgment

This work was funded by TotalEnergies. We thank Celine Boissard, Julie Rousseau, and Sandrine Arii, PLATeforme INstrumentale d'Analysis of IC2MP, for assistance in TEM and XRD analyses and discussions. The authors acknowledge financial support from the European Union (ERDF) and Région Nouvelle Aquitaine. This work pertains to the French government program "Investissements d'Avenir" (EUR INTREE, reference ANR-18-EURE-0010).

References

[1] Klerke A., Christensen C.H., Nørskov J.K., and Vegge T., Ammonia for hydrogen storage: Challenges and opportunities, *J. Mater. Chem*., Vol. 18, pp. 2304–2310, 2008.

[2] Makhloufi C., and Kezibri N., Large-scale decomposition of green ammonia for pure hydrogen production, *Int. J. Hydrogen Energy*, Vol. 46, pp. 34777–34787, 2021.

[3] Sun S., Jiang Q., Zhao D., Cao T., Sha H., Zhang C., Song H., and Da Z., Ammonia as hydrogen carrier: Advances in ammonia decomposition catalysts for promising hydrogen production, *Renew. Sustain. Energy Rev*., Vol. 169, 112918, 2022.

[4] Mukherjee S., Devaguptapu S.V., Sviripa A., Lund C.R.F., and Wu G., Low-temperature ammonia decomposition catalysts for hydrogen generation, *Appl. Catal. B Environ*., Vol. 226, pp. 162–181, 2018.
[5] Comotti M., and Frigo S., Hydrogen generation system for ammonia–hydrogen fuelled internal combustion engines, *Int. J. Hydrogen Energy*, Vol. 40, pp.10673–10686, 2015.
[6] Silva H., Morten M.G., Fiordaliso E., Damsgaard C., Gundlac C, Kasama T., Chorkendorff I., and Chakraborty D., Synthesis and Characterization of FeNi/γ-Al_2O_3 egg-shell catalyst for h_2 generation by ammonia decomposition, *Appl. Catal. A*., Vol. 505, pp. 548–556, 2015.
[7] Huihuang F., Simson W., Tugce A., Jianwei Z., Fellowes J., Ho P.L., Chee K., Large A., Held G., Kato R., Suenaga K., Ira Y., Reyes A., Viet Thang H, Chen H.Y.T., and Edman Tsang S.C., Dispersed surface Ru ensembles on MgO(111) for catalytic ammonia decomposition, *Nature Commun*., Vol. 14, 647, 2023.
[8] Prieto G., Takashima K., Mizuno A., Gay C., and Prieto O., Review about ammonia generation in non-thermal plasma reactors, *Int. J. Plasma Environ. Sci. Technol.*, Vol. 11, pp. 69–80, 2017.
[9] Andersen J.A., Christensen J.M., Ostberg M., Bogaerts A., and Jensen A.D., Plasma-catalytic ammonia decomposition using a packed-bed dielectric barrier discharge reactor, *Int. J. of Hydrogen Energy*, Vol. 47: pp. 32081–32091, 2022.
[10] Hisai Y., Ma Q., Qureishy T., Watanabe T., Higo T., Norby T., and Sekine Y., Enhanced activity of catalysts on substrates with surface protonic current in an electrical field –a review, *Chem. Commun*. Vol. 57, pp. 5737–5749, 2021.
[11] Tanaka K., Sekine Y., Oshima K., Tanaka Y., Matsukata M., and Kikuchi E., Catalytic oxidative coupling of methane assisted by electric power over a semiconductor catalyst, *Chem Lett*., Vol.41, pp. 351–353, 2012.
[12] Maslova V., Fourré E., Veryasov G., Nesterenko N., Grishin A., Louste C., Nassar M., Guignard N., Arrii S., and Batiot-Dupeyrat C., Ammonia decomposition in electric field over Ce-based materials, *ChemCatChem*, Vol. 15 (4), e202201626, 2023
[13] Kanai S., Nagahara I., Kita Y., Kamata K., Hara M.A. Bbifunctional cerium phosphate catalyst for chemoselective acetalization, *Chem. Sci.,* Vol. 8, pp. 3146–3153, 2017.
[14] Stere C.E., Anderson J.A., Chansai S., Delgado J.J., Graham A.G., Hardacre C., Taylor S.F.R., Tu X., Wang Z., Yang H., Non-thermal plasma activation of gold-based catalysts for low-temperature water-gas shift catalysis, *Angew. Chemie - Int. Ed*., Vol. 56, pp. 5579–5583, 2017.
[15] Kim H.H., Abdelaziz A.A., Teramoto Y., Nozaki T., Hensel K., Mok Y.S., Saud S., Nguyen D.B., Lee D.H., Kang W.S., Interim report of plasma catalysis: Footprints in the past and blueprints for the future, *Int. J. Plasma Environ. Sci. Technol*., Vol.15, e01004, 2021.
[16] Sato A., Ogo S., Kamata K., Takeno Y., Yabe T., Yamamoto T., Matsumura S., Hara M., Sekine Y., Ambient-temperature oxidative coupling of methane in an electric field by a cerium phosphate nanorod catalyst, *Chem. Comm.,* Vol. 55, pp. 4019–4022, 2019.
[17] Fateev A., Leipold F., Kusano Y., Stenum B., Tsakadze E., and Bindslev H., Plasma chemistry in an atmospheric pressure Ar/NH_3 dielectric barrier discharge, *Plasma Process. Polym*., Vol. 2, pp. 193–200, 2005.
[18] Rossignol S., Madier Y., and Duprez D., Preparation of zirconia–ceria materials by soft chemistry, *Catal. Today*, Vol. 50, pp. 261–270, 1999.
[19] Reddy A.S., Chen C.Y., Chen C.C, Chien S.H., Lin C.J., Lin K.H, Chen C.L., and Chang S.C., Synthesis and characterization of Fe/CeO_2 catalysts: Epoxidation of cyclohexene, *J. Mol. Catal. A Chem.,* Vol. 318, pp. 60–67, 2010.
[20] Lucentini I., Garcia X., Vendrell X., and Llorca J., Review of the decomposition of ammonia to generate hydrogen, *Ind. Eng. Chem. Res*., Vol. 60, pp. 18560–18611, 2021.
[21] Ilieva L., Pantaleo G., Ivanov I., Venezia A.M., and Andreeva D., Gold catalysts supported on CeO_2 and CeO_2-Al_2O_3 for NOx reduction by CO, *Appl. Catal. B*, Vol 65, pp. 101–109, 2006.
[22] Sekine Y., and Manabe R., Reaction mechanism of low-temperature catalysis by surface protonics in an electric field, *Faraday Discuss*. Vol. 229, pp. 341–358, 2021.
[23] Navarro-Jaén S., Luis F., Bobadilla F., Romero-Sarria F., Laguna O.H., Bion N., and Odriozola J.A., Evaluation of the oxygen mobility in $CePO_4$-supported catalysts: mechanistic implications on the WGS reaction, *J. Phys. Chem. C*, Vol. 124, pp. 16391–16401, 2020.
[24] Oshima K., Shinagawa T., Nogami Y., Manabe R., Ogo S., Y., and Sekine Y., Low temperature catalytic reverse water gas shift reaction assisted by an electric field, *Catal. Today,* Vol. 232, pp. 27–32, 2014.
[25] Wang W., Kim H.H., Van Laer K., and Bogaerts A., Streamer propagation in a packed bed plasma reactor for plasma catalysis applications, *Chem. Eng. J*., Vol. 334, pp. 2467–2479, 2018.